Recent JET Experiments on Alfvén Eigenmodes with Intermediate Toroidal Mode Numbers: Measurements and Modelling of n=3 Toroidal Alfvén Eigenmodes with the TAEFL code [+]

D.Testa[1], D.Spong[2], T.Panis[1], P.Blanchard[1,3], A.Fasoli[1], and JET-EFDA contributors*
JET-EFDA, Culham Science Centre, Abingdon, OX14 3DB, UK

1) Ecole Polytechnique Fédérale de Lausanne (EPFL), Centre de Recherches en Physique des Plasmas (CRPP), Association EURATOM – Confédération Suisse, Lausanne, CH
2) Oak Ridge National Laboratory, Fusion Energy Theory Group, Oak Ridge, USA
3) EFDA-CSU, Culham Science Centre, Abingdon, UK

[+] this contribution is based on a IAEA-FEC-2010 conference presentation, paper EXW/P7-27
e-mail contact of corresponding author: duccio.testa@epfl.ch
classification scheme: D0, Te.

Abstract. This paper reports the results of recent experiments performed on the JET tokamak on Alfvén Eigenmodes (AEs) with toroidal mode number (n) in the range n=3-15. The stability properties of these medium-n AEs are investigated experimentally using a new set of compact in-vessel antennas, providing a direct and real-time measurement of the frequency, damping rate and amplitude for each individual toroidal mode number. We report here the quantitative analysis of the measurements of the damping rate for stable n=3 Toroidal AEs as function of the edge plasma elongation, and the theoretical analysis of this data with the TAEFL code. The TAEFL results are in excellent qualitative agreement with the measurements, reproducing well the experimental scaling of increasing damping rate vs. increasing edge elongation, and in many cases are also quantitatively correct, with a difference with respect to the measurements below 30%, particularly for magnetic configurations that have a larger edge magnetic shear.

*Appendix of F.Romanelli, paper OV1/3, 23rd IAEA Fusion Energy Conference, Daejon, Republic of Korea, 11-16 October 2010.

1. Introduction and Background.

The stability of Alfvén Eigenmodes (AEs) [1] and the effect of these modes on the energy and spatial distribution of fast ions, including fusion generated alpha particles, are among the most important issues for the operation of burning plasma experiments such as ITER. Of particular interest are AEs with toroidal mode number (n) in the range n~3-20, as these are expected to interact most strongly with the alpha particles [2, 3]. The stability of these medium-n AEs is investigated experimentally in JET using an active system (the so-called Alfvén Eigenmodes Active Diagnostic, AEAD) based on a set of eight compact in-vessel antennas and real-time detection and discrimination of the individual toroidal mode number (n-) components in the measured magnetic ($|\omega\delta B_{MEAS}|$) spectrum [4-7]. The AEAD system now routinely provides, also in real-time, a direct measurement of the frequency (f_{MEAS}), damping rate (γ/ω_{MEAS}) and amplitude ($|\delta B_{MEAS}|$: relative value in real-time, absolute value for post-pulse analysis) of the detected modes as function of the dynamical evolution of the background plasma parameters, separately for all the antenna-driven toroidal mode numbers, and for different JET operating scenarios.

Of particular importance for the stability of (fast ion driven) medium-n AEs is the control issue, i.e. what actuators could be used in real-time to prevent these modes from becoming unstable. In JET, the edge plasma shape (hence the edge magnetic shear) have been found to be key ingredients for increasing the damping of stable, antenna-driven low-n (n=1 and n=2) and unstable, fast-ion driven medium-n (n~3-10) [8-12] Toroidal AEs (TAEs). These results suggested that the edge elongation could indeed be effectively used for real-time control of the stability of fast ion driven medium-n AEs. The previous experimental results on JET also motivated further experimental studies on the Alcator C-mod tokamak where it was found, contrary to the JET results, that the damping rate of an n=6 TAE does not change much when the average edge triangularity (δ_{95}) is scanned in the range $0.3<\delta_{95}<0.7$ [13].

The new AEAD system on JET has allowed a more systematic study of the stability of medium-n AEs in limited and X-point plasmas, and the initial results of these studies have been reported in [6, 7, 14]. It was experimentally found that the damping rate of n=3 and n=7 TAEs show an almost linear increase as a function of the edge elongation (κ_{95}), in the range $1.25<\kappa_{95}<1.65$, i.e. from almost circular to highly shaped plasmas. Specifically, it is important to note that the highest relative variation in the measured damping rates was obtained for a relatively small variation in the edge elongation of the order of 5%, i.e. between κ_{95}~1.40 to κ_{95}~1.45. Hence, increasing κ_{95} has in JET the same effect on the damping rate of these medium-n TAEs as on the n=1 and the n=2 TAEs. These measurements were also theoretically analysed using the LEMan code [15, 16]. These LEMan results, already reported in [6, 14], reproduce qualitatively and quantitatively within a factor

2 the experimental scaling of γ/ω_{MEAS} as function of κ_{95}. These experimental and theoretical results confirm that the same edge damping mechanisms acting upon global, low-n modes, play a substantial role also for the stability of more core-localised medium-n TAEs, opening interesting perspectives for their real-time control. In this respect, it is important to note that the power supplies for the shaping coils used in JET to change the edge elongation have a response function faster than 10ms, and a similar time scale is also foreseen for the corresponding power supplies in ITER, which indeed should make it possible to fine-tune in real-time the edge shape to affect and control the TAE stability. As observed in JET, an increase of less than 5% around the optimal and pre-defined value of the edge elongation produces a factor ~2→5 increase in the damping rate of TAEs with n=1→10. It is clear from the JET operational experience on advanced tokamak scenarios that such an increase has effectively no impact on the plasma performance, and would still be within the allowed limits on the plasma-wall clearance.

In this paper we focus on a further theoretical analysis of the damping rate measurements for the n=3 TAEs previously reported in [6] using the TAEFL code [17, 18]. As the TAEFL and LEMan estimation of the damping rate of the modes is based on different numerical algorithms, this work is important not only as a code-to-code benchmark, but also in that it indicates whether the essential physics mechanisms are retained in the numerical calculations, irrespective of the actual details of the calculations themselves.

This paper is based on a contribution presented at the 23rd IAEA Fusion Energy Conference [14]. As such, this presentation is organised as follows. Section-2 gives a brief description of the new JET AEAD system. Section-3 reports the experimental measurements of the damping rate for n=3 TAEs, focussing particularly on the dependence vs. the edge elongation. In Section-4 we present the results of the simulations that have been run to model the n=3 data using the TAEFL code. Finally, in Section-5 we present the conclusion of this work and an outline towards future activities. Another contribution presented at the 23rd IAEA Fusion Energy Conference [19] gives additional numerical and more theoretical details on the analysis of the n=3 data performed used other numerical codes in the framework of the ITPA Energetic Particle group work-programme.

2. The new JET Alfvén Eigenmodes Active Diagnostic System.

The general description of the new JET Alfvén Eigenmodes Active Diagnostic (AEAD) system has been presented in [5-7], the active synchronous detection diagnostic technique was first described in [4], and the development of the real-time hardware and software analysis system using the *Sparse Signal Representation* method and the *SparSpec* code [20, 21] has been presented in details in [22-24]. For these reasons, here we only briefly review the main aspects of the AEAD system to provide

a simple reminder of its main capabilities, with the main goal of facilitating the understanding of the experimental results presented in Section-3.

The AEAD system consists principally of three components:

1. the AE exciter, built upon a function generator and an high-power amplifier (5kW, 10A-peak, 700V-peak, 10→500kHz frequency range of operation) connected to a set of up to eight in-vessel antennas, whose aim is to send power into the plasma in order to drive a very small magnetic perturbation, $\max(|\delta B_{DRIVEN}|)\sim 0.1G$ at the plasma edge, i.e. 10^5 times smaller than the typical value of the toroidal magnetic field in JET, $B_{TOR}\sim(1\text{-}3)T$;

2. eight compact, solenoid-like, in-vessel antennas, installed in two groups of four closely-spaced units at two toroidally opposite positions, at the same poloidal location, with the first turn sitting approximately ~45mm behind the line of the poloidal limiters; each antenna has 18 turns in the direction perpendicular to the plasma magnetic surfaces (the solenoid axis), and an extent of approximately 25cm (toroidally) × 27cm (vertically) in the plane facing the plasma; each four-antenna unit occupies a toroidal length of approximately 130cm;

3. a receiver, built upon synchronous detection units, which collects signals from various in-vessel detectors (magnetic pick-up coils, electron cyclotron emission, reflectometry); this receiver is also connected to the real-time AE Local Manager (AELM) to allow the detection and tracking of antenna-driven plasma resonances with different toroidal mode numbers.

Any combination of these eight antennas can be chosen with a ± relative phasing. Hence, due to close spacing between the antennas, a broad toroidal spectrum is always excited for any antenna frequency, comprising many components, usually up to $|n|\sim 30$, of which the higher-n ones are more strongly attenuated as function of the distance from the antennas. To illustrate this result, the flux-surface-averaged radial ($\langle B_{RAD}\rangle$) and poloidal ($\langle B_{POL}\rangle$) components of the antenna-driven magnetic field are shown in fig1 for the JET shot #77788 for different toroidal mode numbers and three time points (t=5.00sec, t=10.50sec and t=14.00sec), corresponding to the beginning, the middle and the end of the edge elongation scan, for which the damping rate measurements will be shown in Section-3. The uncertainty in the calculation of the antenna-driven magnetic field is a combination of the error on the measurement of the antenna current (typically correct within 10%) and on the reconstruction of the equilibrium magnetic geometry, which is used for the flux-surface averaging. In total, we estimate that the relative error on the antenna-driven, flux-surface averaged, radial and poloidal magnetic field does not exceed 10% for the cases considered in this work. Note that up to two orders of magnitude difference in the antenna-driven $\langle B_{RAD}(n)\rangle$ and $\langle B_{POL}(n)\rangle$ is seen between its different n-components up to $|n|\leq 30$ as the plasma background evolves during the

shot, which makes it an essential requirement to be able to discriminate in real-time the different n-components in the measured $|\omega\delta B_{MEAS}|$ spectrum.

Owing to the antenna geometry, a frequency-degenerated spectrum of plasma resonances is routinely obtained, i.e. one where the half-width at half-maximum of the modes (a quantity closely related to the damping rate) is comparable to their separation in frequency. This spectrum is analysed in real-time (and obviously post-pulse as well) by the AELM using a novel method for mode detection and n-number discrimination, based on the *Sparse Signal Representation* theory and the *SparSpec* algorithm [20-24]. The speed and accuracy of the *SparSpec* algorithm has made it possible to deploy it in our plant control software, allowing real-time tracking of the individual n-modes during the evolution of the plasma background on a sub-millisecond time scale, which is fully compatible with the JET real-time signal server hardware and software. An example of this real-time detection and discrimination of the concurrent n=3, n=5 and n=7 Toroidal AEs (TAEs) is shown in fig2 for the JET shot #77788, where the excitation system was configured to drive predominantly n-odd modes, with $\max(|\delta B_{DRIVEN}(n)|)$ in the range $|n|\sim$3-7, and producing a negligible drive for components with $|n|>10$. The analogue signal $|\delta B_{MEAS}|$ shows the amplitude of each individual mode as detected in real-time using *SparSpec*. The digital signals indicate whether detection and tracking of a certain mode has been successful: when the flag is set to high (=1), then the corresponding mode has been correctly detected and tracking is occurring. First, we note that only very few n=even resonances (n=[4, 6, 8]) are detected in real-time (and confirmed by post-pulse analysis: see [23, 24] for further details), compared to the number of n=3, and more generally n=odd, resonances; second, the n=3 mode dominates the detected spectrum, as this is the one for which the AEAD system produces the maximum drive and the plasma produces the maximum response at the magnetic pick-up coils used for this measurement.

3. Measurements of the Damping rate for n=3 Toroidal Alfvén Eigenmodes in JET.

The measurements of the damping rate for medium-n AEs are now being routinely obtained in different JET operating scenarios [6, 7, 14]. An example of these experimental configurations is shown in fig3 for the shot #77788, which has been used for detailed comparisons with theory and models in the framework of the ITPA Energetic Particle Group work-program [19]. This discharge is an example of a series of dedicated experiments where an ohmically heated plasma configuration was designed for a slow edge elongation increase from $\kappa_{95}\sim1.33$ at t=9sec to $\kappa_{95}\sim1.65$ at t=16sec, while the other background plasma parameters, including the safety factor profile, were designed to be kept (and were measured to be) essentially constant. The slow edge elongation scan follows the

usual relaxation of the q-profile occurring in the earlier part of this type of ohmically heated discharges, from q_0~1.05 and q_{95}~4.2 at t=5sec to q_0~0.85 and q_{95}~3.85 at t=9.5sec.

Figure3 shows the time evolution of the main background plasma parameters for the JET shot #77788: the toroidal field on the magnetic axis is B_ϕ=2.7T, the plasma current is I_p=2MA. The central frequency of the n=1 TAE gap at s=$\sqrt{\psi_N}$=0 (label fRTn1 in fig3) is calculated in real-time by the AELM (assuming q_{TAE}=(2m+1)/2n=1.5, R=3m, and using the line-averaged value of the electron density in the plasma core from the interferometer measurements) and post-pulse (label fAEn1 in fig3) using the EFIT measurement of the q-profile in the plasma core and the measurement of the core electron density obtained via the High-Resolution Thomson Scattering diagnostic. Note that 100ms-long NBI diagnostic blips were used to provide MSE measurements for the q-profile (which are very similar to the EFIT data) and charge-exchange measurements for the ion temperature (giving $T_i(s)$~$T_e(s)$) and the toroidal rotation frequency profiles (giving $f_{ROT}(s)$~1kHz). Note also that great care was taken in preparing this series of experiments so that there would be only very minimal differences in the background plasma profiles as the discharges evolves (as clearly shown later in fig4), with the notable exception of the edge shaping parameters (elongation and triangularity), so that their effect on the damping rate of medium-n TAEs could be clearly identified and isolated experimentally.

In the discharge #77788, the antenna-plasma distance was minimized and the plasma configuration was optimized in order to achieve a good antenna-plasma coupling. The configuration used for the antenna excitation was also optimized with the use of a matching unit in order to achieve maximum antenna currents with as minimum a ripple as possible in the frequency range $150<f_{ANT}(kHz)<250$, giving I_{ANT}~5.5A±2A on the four active antennas selected for this discharge. As indicated before, the excitation system was configured to drive predominantly n-odd modes, with max($|\delta B_{DRIVEN}(n)|$) in the range |n|~3-7, and producing a negligible drive for components with |n|>10.

Figure4 shows the profiles of the main background plasma parameters at the time points used for the TAEFL simulations that will be presented in Section-4. The equilibrium current and shaping data have been evaluated using the EFIT code [25]; the electron density and temperature are taken from the HRTS measurements. The typical uncertainty on the $n_e(s)$ and $T_e(s)$ profile is of the order of 5→10% across the entire poloidal cross-section: this was evaluated combining the error bar on the actual HRTS data, with the scatter in the data that can be inferred by comparing the HRTS data with the FIR interferometer and LIDAR data for the electron density profile and the ECE and LIDAR data for the electron temperature profile. The typical uncertainty on the q-profile can also be taken to be of the order of 5→10% across the entire poloidal cross-section. Both sets of error bars are not shown in fig4 to avoid excessive cluttering. Note that the profiles for the main

background plasma parameters (electron density and temperature, q-profile) are indeed very similar, and in fact almost indistinguishable, throughout the edge elongation scan, whereas the change in the edge elongation (and the ensuing changes in the edge triangularity) are very clearly seen to appear from around mid-radius, i.e. for s>0.65, as the discharge evolves.

Several TAE modes are successfully identified in #77788 throughout the discharge, both in real-time and with the post-pulse analysis, as shown in fig5. The typical uncertainties on the measured mode frequency and damping rate are below <1kHz and 15% for the measurements presented here (see [6] for further details). Note that modes with the same toroidal mode number are detected at almost the same time at different frequencies within the TAE gap and with very different damping rate, hence the importance of being able to track in real-time the evolution of one specific single n-mode. Focusing on the n=3 TAEs that have been the subject of extensive theoretical modelling, of which the TAEFL runs will be presented in Section-4, we note two distinct effects. First, during the q-profile relaxation in the initial phase of the discharge, i.e. in the time interval 4.5<t(sec)<9.5, the damping rate of n=3 TAEs increases from γ/ω_{MEAS}~0.3% to γ/ω_{MEAS}~2%. The second effect is the variation of the n=3 damping rate with the increasing edge elongation (κ_{95}: from ~1.25 to ~1.65) and edge magnetic shear (s_{95}: from ~3.2 to ~5.5), which occur concurrently with a relatively minor increase in the value of the edge safety factor (q_{95}: from ~3.85 to ~4.15). During this phase, i.e. in the time interval 9<t(sec)>16.5, the damping rate increases from γ/ω_{MEAS}~2% to γ/ω_{MEAS}~4.5%. This experimental scaling of increasing damping rate vs. increasing edge elongation agrees very well with previous JET data for low-n TAEs [8]. Note that the last few measurement points, for t>15.5sec, have been obtained after an X-point is formed in the lower half of the plasma. Note also that, operationally, changes in the edge elongation are directly related to changes in the current applied to the shaping coils, and the changes in the edge safety factor, hence in the edge magnetic shear, correspondingly ensue from the increase in the edge elongation.

Looking at fig5, it is immediately apparent that various modes with the same toroidal mode number but with very different damping rates are detected at almost the same time at different frequencies within the TAE gap. Furthermore, modes with different toroidal mode numbers but almost the same frequency are also detected at almost the same time. Figure6 illustrate this finding for the specific case of the n=+3 TAE, whose frequency and damping rate are plotted as function of the edge elongation. For comparison purposes, the frequency of the n=+7, n=-1 and n=-3 TAEs is also shown, to demonstrate their close proximity, which makes it essential to have a very accurate real-time (and post-pulse) mode discrimination and tracking algorithm if any useful comparisons with theory is to be obtained, as for such work it is essential to be able to track in real-time the *same* n-mode during the evolution of the plasma background, and to select the *same* n-mode for the

simulations. This essential feature is achieved using the world-wide unique real-time mode discrimination and tracking algorithm we routinely employ in the JET AEAD system [23, 24].

4. Modelling of the n=3 Damping Rate Measurements with the TAEFL Code.

The study of collective instabilities, and particularly AEs, driven by the fast ion populations is of paramount importance for the successful operation of the forthcoming burning plasmas experiments aimed at achieving a net fusion energy gain. Hence, Alfvén waves and AEs have been the subject of many studies, both theoretical and experimental [26-31]. However, many aspects of the interpretation of the damping rate measurements are still in need of further analysis, specifically including code-to-code vs. actual measurement comparisons, before the currently available models can be considered to be able to provide accurate predictions for future devices such as ITER.

The JET measurements of the damping rate for AEs with intermediate toroidal mode numbers, together with the capability of obtaining accurate equilibrium reconstruction and measurements of the background plasma parameters such as the density, the temperature and the q-profile, provide a very suitable platform for developing code-to-code comparisons aimed at assessing which physics and computational elements of the different codes are best adapted to explain the JET data, with a view to provide accurate predictions for future burning plasma experiments such as ITER.

The JET shot #77788 was used for such code-to-code vs. measurements comparison studies within the ITPA working group on Energetic Particles. This exercise included the contribution of various numerical codes, ranging from perturbative MHD models such as those employed in CASTOR(-K) [32, 33] and NOVA(-K) [34, 35], to those employing a warm dielectric tensor model like LEMan [15, 16] to fully gyro-fluid models such as that used in TAEFL [17, 18] and linear gyro-kinetic models as that employed in LIGKA [36]. Many aspects of these studies have been presented elsewhere [7, 8, 14, 19]; therefore, here we specifically focus only on the analysis performed with the TAEFL code.

The TAEFL code [17, 18] is a reduced MHD initial value code that uses gyrofluid closure techniques for the energetic ions to incorporate the Landau resonance effects that destabilize Alfvén modes. Since only unstable modes can be analyzed by TAEFL, the technique used in this comparison with the JET data for stable n=3 modes, was to start with an unstable Alfvén mode, vary the fast ion drive and extrapolate back to zero drive in order to determine an effective damping rate. Fast ion profiles/parameters are chosen that lead to a mode very close to the frequency excited by the antenna, i.e. within a few percents of the measured frequency (typically less than 5kHz difference between the measured and the predicted frequency). This model incorporates ion/electron Landau damping, continuum damping and radiative damping (due to finite ion Larmor radius)

effects. It uses Fourier spectral representations in the poloidal and toroidal directions and finite differences in the direction normal to the flux surfaces. The TAEFL simulations of JET plasmas used 300 radial points and 26 Fourier modes (m=0→25). TAEFL is currently limited to up-down symmetric, but non-circular magnetic equilibria; hence, the JET equilibria used in this study were modified to be up-down symmetric, but maintaining a similar non-circular shaping with respect to the elongation and the triangularity. Seven time points have been selected for comparison with the TAEFL code, spanning the entire range of the damping rate measurements for the n=3 TAEs in #77788, from the initial phase of the discharge when the measured damping rate is very low (γ/ω_{MEAS}~0.5%) to the X-point phase later in the discharge, when the damping rate is very large (γ/ω_{MEAS}~5.5%).

Figure7(a-c) shows the radial Eigenfunction and the 2D contour plot of the n=3 Eigenmode calculated by the TAEFL code for the JET shot #77788 at three representative time points during the elongation scan: t=10.248sec (fig7a), t=14.261sec (fig7b) and t=15.835sec (fig7c). The profiles of the background plasma parameters (electron density and temperature, q-profile from EFIT, elongation and averaged up/down triangularity) are also shown for comparison purposes. As shown in more details in [14, 19], it is very important to note that, despite the differences between the codes, the mode frequency and the radial Eigenfunctions computed by the TAEFL code are in very good agreement with those computed by the LEMan, LIGKA, NOVA(-K) and CASTOR(-K) codes. This indicates not only a very good understanding of the main and most robust physics mechanisms contributing to determining the existence and frequency localisation of these medium-n AEs, but also of the effect that the differences between the various codes and models, particularly that used for the antenna, can have on the predictions for ITER [19]. Note however that direct measurements of the radial Eigenfunction for stable AEs have only rarely been obtained, and specifically in JET, because of too a poor sensitivity of the internal fluctuation diagnostics used for this purpose.

Figure8 shows the measurements of the damping rate for the n=3 TAEs selected for this comparison as function of the edge elongation in ohmic plasmas, together with the results of the simulations performed with TAEFL and some additional points from LEMan [6, 14] and CASTOR [14, 19] for illustrative purposes. For the measurements for the JET shot #77788, the vertical error bar indicate the actual error on this data, whereas the error bar for the data points for other JET shots also include the scatter in the damping rate measurements obtained for these κ_{95} points. This scatter then includes not only the estimated error on the individual γ/ω_{MEAS} measurements, but also the variation observed for different JET discharges and background plasma parameters (absolute value and profiles) in γ/ω_{MEAS} for n=3 modes at similar frequency within the TAE gap.

First, we note in fig8 that the trend of increasing damping rate for increasing edge elongation is qualitatively very well reproduced by TAEFL. Second, the TAEFL results are also in very good quantitative agreement with the measurements for relative high values of the edge elongation (κ_{95}>1.40), corresponding also to a larger edge magnetic shear, whereas the discrepancy at lower values of κ_{95} is somewhat larger. Third, comparing the TAEFL with the LEMan results, we note again a rather good agreement between these two very different codes, that both include kinetic effects, which is very promising for assessing the stability of medium-n TAEs in future burning plasmas such as ITER. Conversely, there is a much larger discrepancy between the TAEFL and the CASTOR code, indicating that this fluid code, that includes only continuum damping, does not always capture the essential elements need to evaluate the damping of medium-n TAEs, Hence, combining the results reported here with those previously reported for the LEMan, CASTOR(-K) and LIGKA codes, the TAEFL simulations have clearly demonstrated the need to include in the calculations a large number of poloidal harmonics, and that continuum damping is not the only mechanism accounting for the measured damping rate for these modes.

Furthermore, it is important to note that TAEFL is the only model used in the ITPA exercise that attempts to infer damping rates by extrapolating unstable growth rates back to zero drive using non-perturbative Eigenfunctions. On the one hand, this may not be the most precise way to model the JET experimental damping measurements, since the modes observed in the experiment are antenna-driven, stable modes, not fast-ion driven instabilities. However, as shown here, the fact that the damping rate variation of the antenna-driven, stable modes compares very well with that for the calculated unstable modes, provides strong support for the relevance of this method to extract equivalent damping rate measurements for unstable AEs. This is particularly important because at this time there is no experimental technique available to directly measure the damping rate of unstable AEs, therefore detailed simulations are necessary to make this connection, and the successful comparison with the JET data reported here proves that this is a valid approach.

5. Conclusions.

A new algorithm, based on the Sparse Representation of signals, has been developed and fully implemented to discriminate in real-time the different toroidal components in the plasma response to the multi-components, frequency-degenerate, magnetic field spectrum driven by the new AE antennas in JET. The quantitative analysis of the damping rate measurements obtained in JET for medium-n TAEs has confirmed the experimental scaling of an increase in γ/ω for increasing edge elongation. This scaling agrees very well with previous JET data for low-n TAEs. These new JET experimental results further confirm the possibility of using the edge shape parameters as a real-

time actuator for the control of the AE stability in future burning plasma experiments. Detailed simulations performed with the TAEFL code are in good qualitative (trend well reproduced) and quantitative (within a factor ~2) agreement with the measurement of the damping rate of n=3 TAEs as function of the edge elongation.

Acknowledgements.

This work was supported by EURATOM under the contract of Association with CRPP-EPFL, and was carried out within the framework of the European Fusion Development Agreement. This work was also partly supported by the Swiss National Science Foundation. The views and opinions expressed herein do not necessarily reflect those of the European Commission. The Authors would also like to thank the various members of the CRPP, MIT and JET staff that have contributed to the design, installation, commissioning and routine operation of the new TAE antenna system, and particularly A.Goodyear (CCFE), H.Carfantan (LATT) and M.Tsalas (JET-EFDA-CSU). The Authors would also like to thank the Reviewers for their useful comments and suggestions to the first draft of this paper.

References.

1. K.-L.Wong, Plasma Phys. Control. Fusion **41** (1999), R1.
2. W.W.Heidbrink, Phys. Plasmas **9**(5) (2002), 2113.
3. G.Vlad, S.Briguglio, G.Fogaccia, F.Zonca, Nucl. Fusion **46** (2006), 1.
4. A.Fasoli et al., Phys. Rev. Lett. **75**(4) (1995), 645.
5. D.Testa et al., *The new Alfvén Wave Active Excitation System at JET*, Proceedings 23rd SOFT Conference (2004); weblink: http://infoscience.epfl.ch/record/143354.
6. D.Testa et al., Nucl. Fusion **50** (2010), 084010.
7. T.Panis, D.Testa et al., Nucl. Fusion **50** (2010), 084019.
8. D.Testa, A.Fasoli, Nucl. Fusion **41** (2001), 809.
9. D.Testa, A.Fasoli, A.Jaun, Nucl. Fusion **43** (2003), 724.
10. D.Testa, A.Fasoli, D.Borba et al., Plasma Phys. Control. Fusion **46** (2004), S59.
11. A.Jaun, A.Fasoli, J.Vaclavik, L.Villard, Nucl. Fusion **40** (2000), 1343.
12. A.Fasoli, A.Jaun, D.Testa, Phys. Lett. **A265** (2000), 288.
13. J.A.Snipes, N.Basse, C.Boswell et al., Phys. Plasmas **12** (2005), 056102.
14. D.Testa et al., *Recent JET Experiments on Alfvén Eigenmodes with Intermediate Toroidal Mode Numbers: Measurements and Modelling*, Paper EXW/P7-27, 23rd IAEA Fusion Energy Conference, Daejon, Republic of Korea, 11-16 October 2010; weblink: http://infoscience.epfl.ch/record/153045.
15. P.Popovich, W.A.Cooper, L.Villard, Comput. Phys. Comm. **175** (2006), 250.
16. N.Mellet, CRPP-EPFL PhD Thesis (weblink: http://library.epfl.ch/theses/?nr=4398); submitted for publication in Computer Physics Communication, October 2010.
17. D.A.Spong, B.A.Carreras, C.L.Hedrick, Phys Fluids B-Plasma **4**, 3316 (1992).
18. D.A.Spong, B.A.Carreras, C.L.Hedrick, Phys Plasmas **1**, 1503 (1994).
19. P.Lauber, S.Günter et al., *The Influence of Plasma Shaping on the Damping of Toroidal Alfvén Eigenmodes*, Paper THW/P7-08, 23rd IAEA Fusion Energy Conference, Daejeon, Republic of Korea, 11-16 October 2010); weblink: http://infoscience.epfl.ch/record/164163.
20. S.Bourguignon, H.Carfantan, T.Böhm, Astronomy and Astrophysics **462** (2007), 379.
21. S.Bourguignon, H.Carfantan, J.Idier, IEEE Journal of Selected Topics in Sig. Proc. **1** (2007), 4; doi: 10.1109/JSTSP.2007.910275.
22. A.Klein, H.Carfantan, D.Testa et al., Plasma Phys. Control. Fusion **50** (2008), 125005.
23. D.Testa et al., EuroPhysics Letters **92** (2010), 50001; doi: 10.1209/0295-5075/92/50001.
24. D.Testa et al., *The JET Alfvén Eigenmode Local Manager for the real-time detection and tracking of a frequency-degenerate spectrum of MHD instabilities*, submitted to Fusion Engineering and Design, August 2010; weblink: http://infoscience.epfl.ch/record/164211.

25. L.L.Lao, H.St-John, R.D.Stambaugh, A.G.Kellman, W.Pfeiffer. Nucl. Fusion **25** (1985), 1611.
26. C.Z.Cheng, L.Chen, M.S.Chance, Annals of Physics **161** (1985), 21.
27. A.Fasoli et al., Phys. Plasmas **7** (2000), 1816-1824.
28. S.Sharapov et al Nucl. Fus. **40** (2000), 1363-1381.
29. S.Sharapov et al., Fusion Science and Technology **53**(4) (2008), 989-1022; and references therein; weblink: http://epubs.ans.org/?a=1745.
30. A.Fasoli et al., *Physics of Energetic Ions*, "Progress in the ITER Physics Basis", Nucl. Fusion **47** (2007), S264-S284; and references therein.
31. W.W.Heidbrink, Phys. Plasmas **15** (2008), 055501.
32. W.Kerner, J.P.Goedbloed et al., Journal of Computational Physics **142** (1998), 271.
33. G.T.A.Huysmans et al., Phys. Fluids **B5** (1993), 1545.
34. C.Z.Cheng, Phys. Reports **211** (1992), 1.
35. N.N.Gorelenkov, C.Z.Cheng, G.Y.Fu, Phys. Plasmas **6** (1999), 2802.
36. Ph.Lauber, S.Günter et al., Journal Computational Physics **226** (2007), 447.

Figure Captions.

Figure1(a,b,c). The calculated flux-surface-averaged poloidal ($<B_{POL}(n,t)>$: top frame) and radial ($<B_{RAD}(n,t)>$: bottom frame) components of the antenna-driven magnetic field for the JET shot #77788 for different toroidal mode numbers and three time points, plotted as function of the radial coordinate $s=\sqrt{\psi_N}$, corresponding to the square root of the normalized poloidal flux.

Figure2. Real-time discrimination between the different toroidal components in the frequency-degenerated AE spectrum driven by the new antennas for the JET shot #77788; the calculation is performed using a CPU-time of <600μs within each 1ms AELM clock cycle.

Figure3. The main background plasma parameters for the JET shot #77788. The labels f-ANT, fRTn1 and fAEn1 indicate, respectively, the antenna driving frequency, and the central frequency of the n=1 TAE gap at $s=\sqrt{\psi_N}=0$ calculated in real-time by the AELM and post-pulse. Here q is the safety factor and s the magnetic shear, β_N is the normalized plasma beta and P_{NBI} is the NBI blip power, κ is the elongation, δ is the averaged up/down triangularity, li is the plasma internal inductance, T_e and T_i are the electron and ion temperatures, n_e is the plasma density, zeff is the effective charge, with the suffixes "0", "95" and "<>" indicating the core, edge and volume-averaged values, respectively. For illustrative purposes, the signal from one of the synchronously acquired magnetic pick-up coils is also shown in the top frame.

Figure4. The profiles of the main background plasma parameters at the time points used for the TAEFL simulations (note that $T_i \sim Te$).

Figure5. Measurement of the mode frequency (f_{MEAS}) and damping rate (γ/ω_{MEAS}) for individual toroidal mode numbers for the JET shot #77788 as function of the evolution of the edge magnetic shear (s_{95}) and elongation (κ_{95}). The various n-modes that have been detected are ordered in the plot according to decreasing residue amplitude, as measured using magnetic pick-up coils mounted on the vessel wall on the low-field side.

Figure6. Frequency and damping rate for the n=3 TAEs detected in the JET shot #77788, plotted as function of the edge elongation κ_{95}, that were selected for the TAEFL analysis.

Figure7. The radial Eigenfunction (top left frame, expressed in terms of the electrostatic potential $\Phi_{mn}(s)$), the 2D contour plot (top right frame) of the n=3 Eigenmode as calculated by the TAEFL code and the background plasma profiles (bottom frame) in the JET shot #77788at t=10.248sec (fig7a), t=14.261sec (fig7b) and t=15.835sec (fig7c). The radial coordinate is $s=\sqrt{\psi_N}$ as in fig4.

Figure8. Damping rate data for n=3 TAEs as function of κ_{95}, compared with the results of the TAEFL simulations, and some additional points from LEMan and CASTOR.

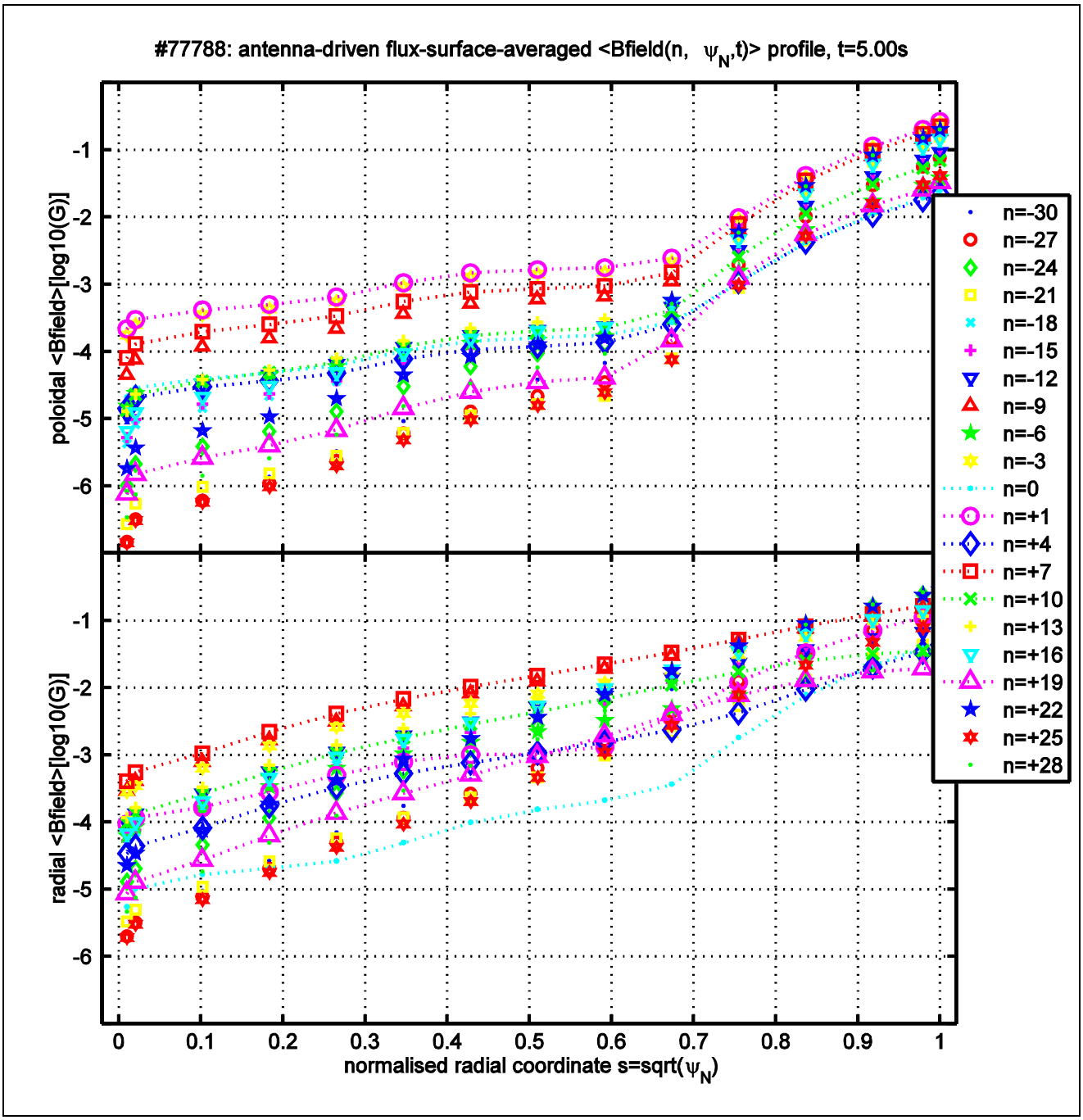

D.Testa, Paper NF2011, Figure1a

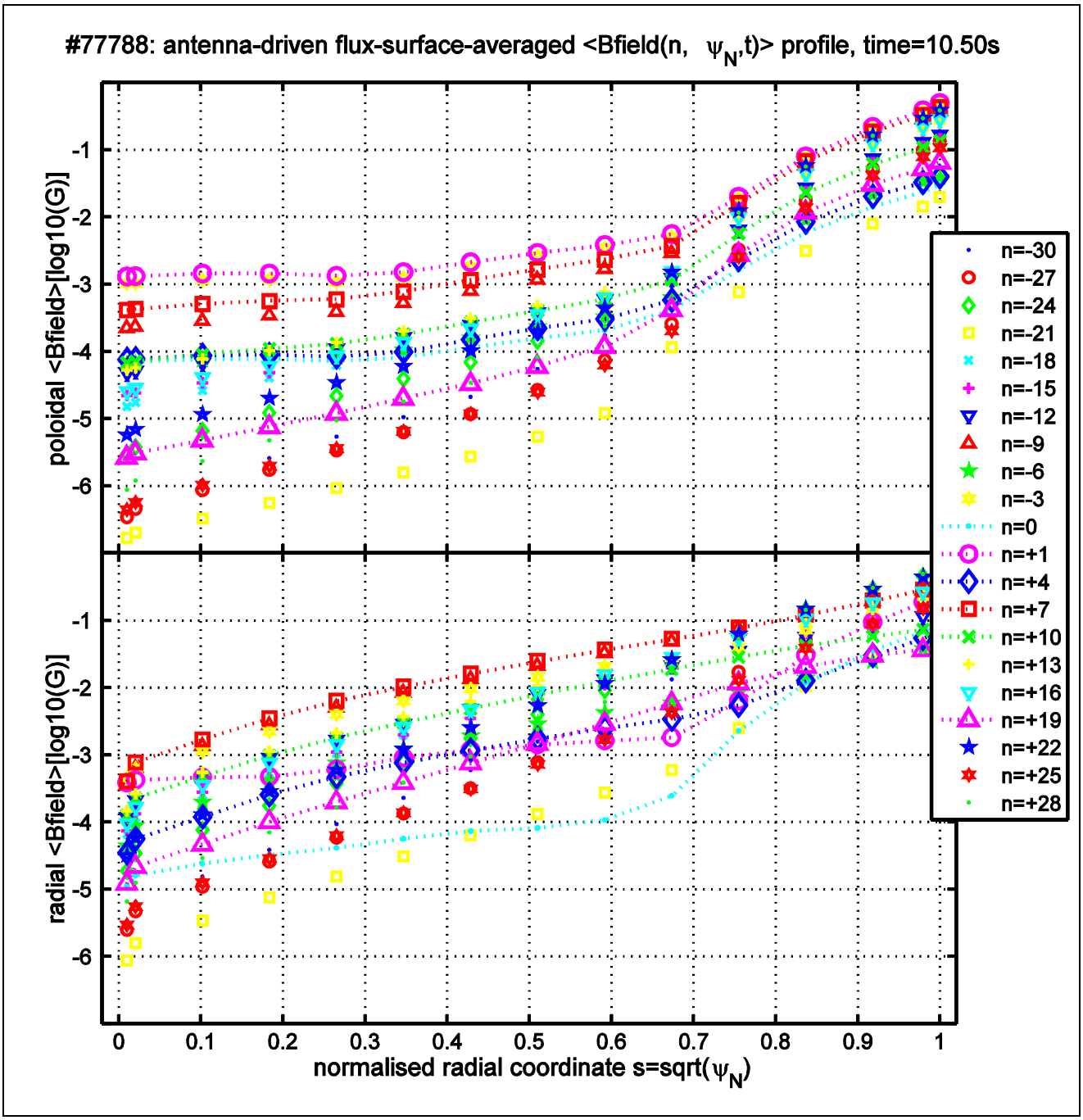

D.Testa, Paper NF2011, Figure1b

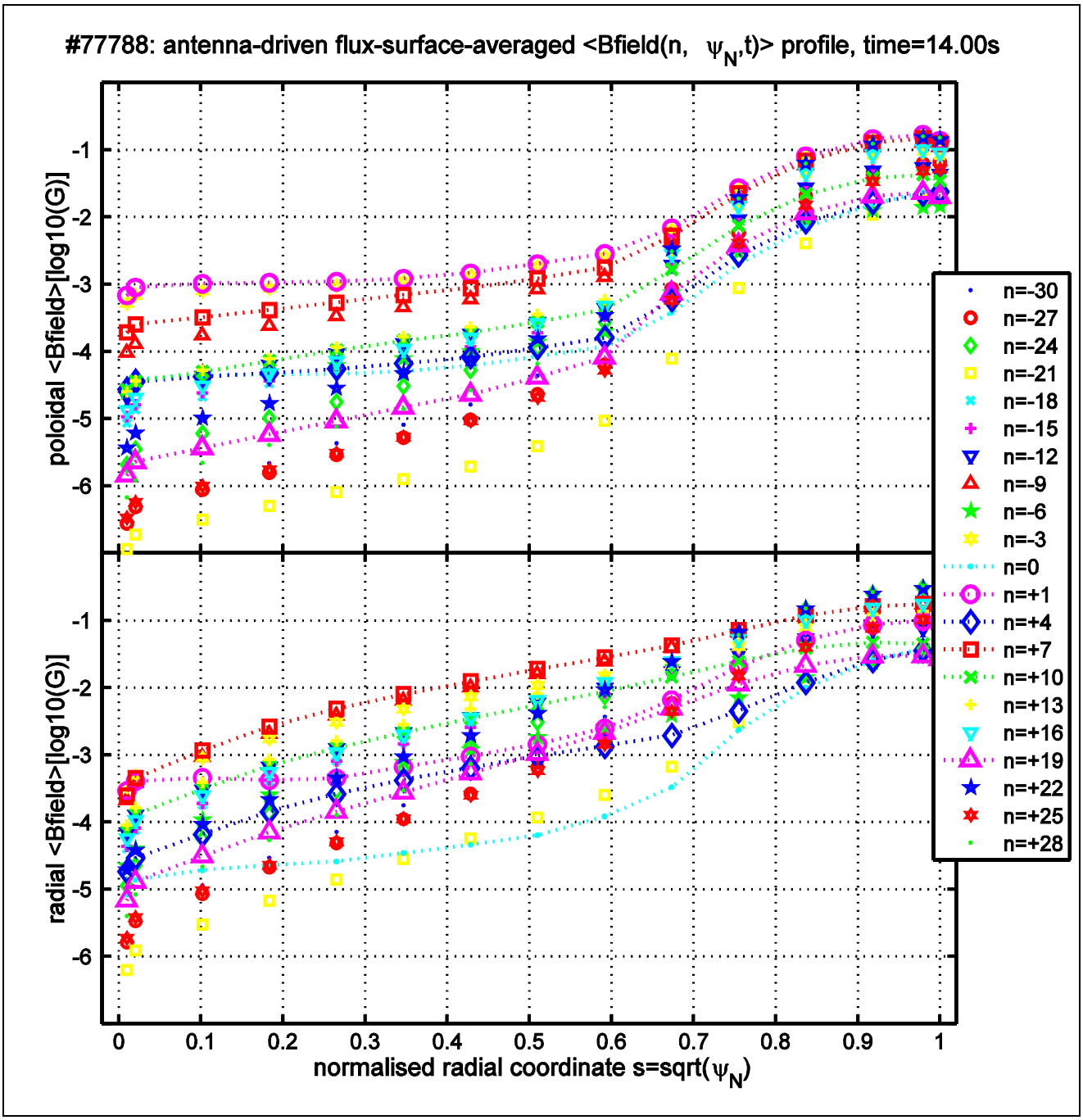

D.Testa, Paper NF2011, Figure1c

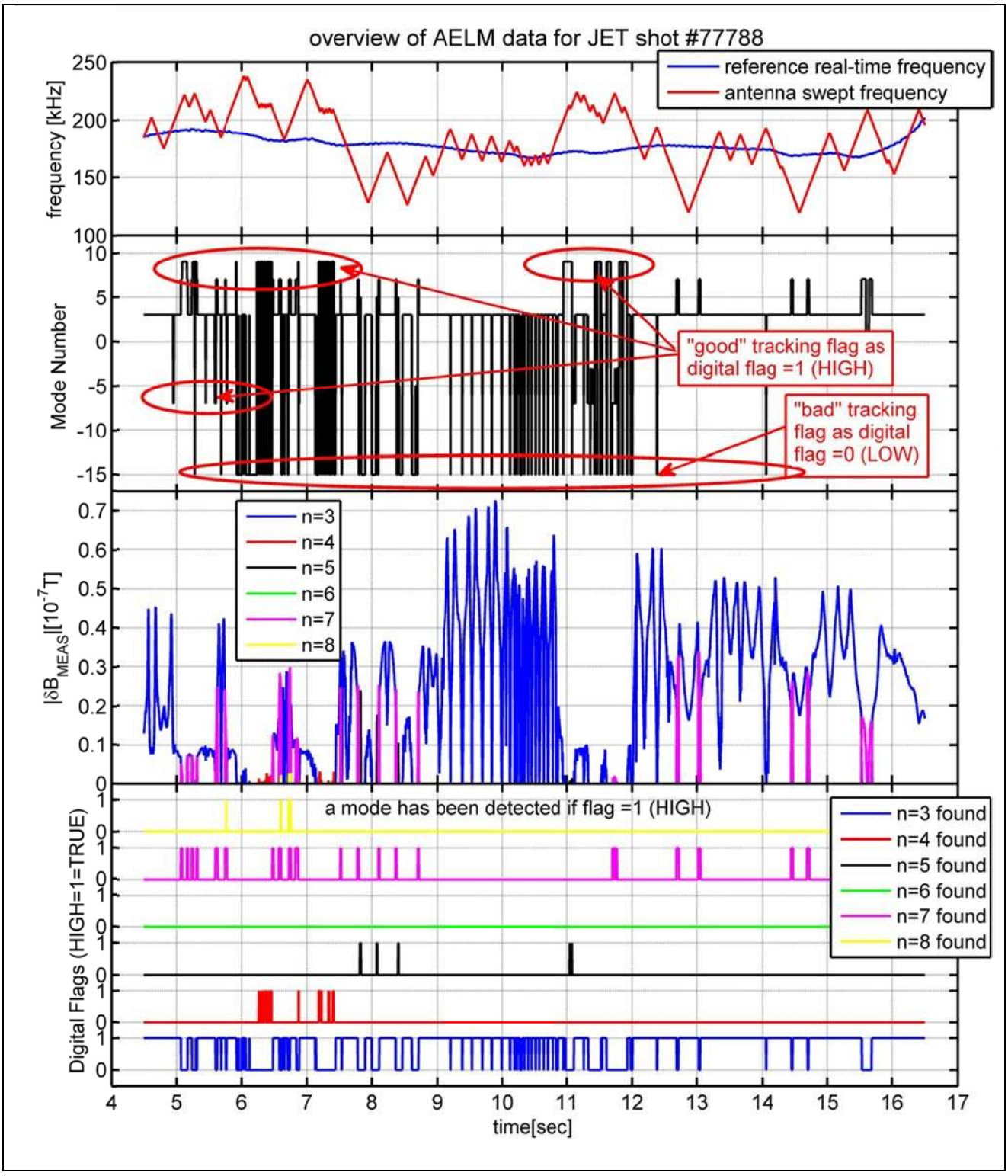

D.Testa, Paper NF2011, Figure2

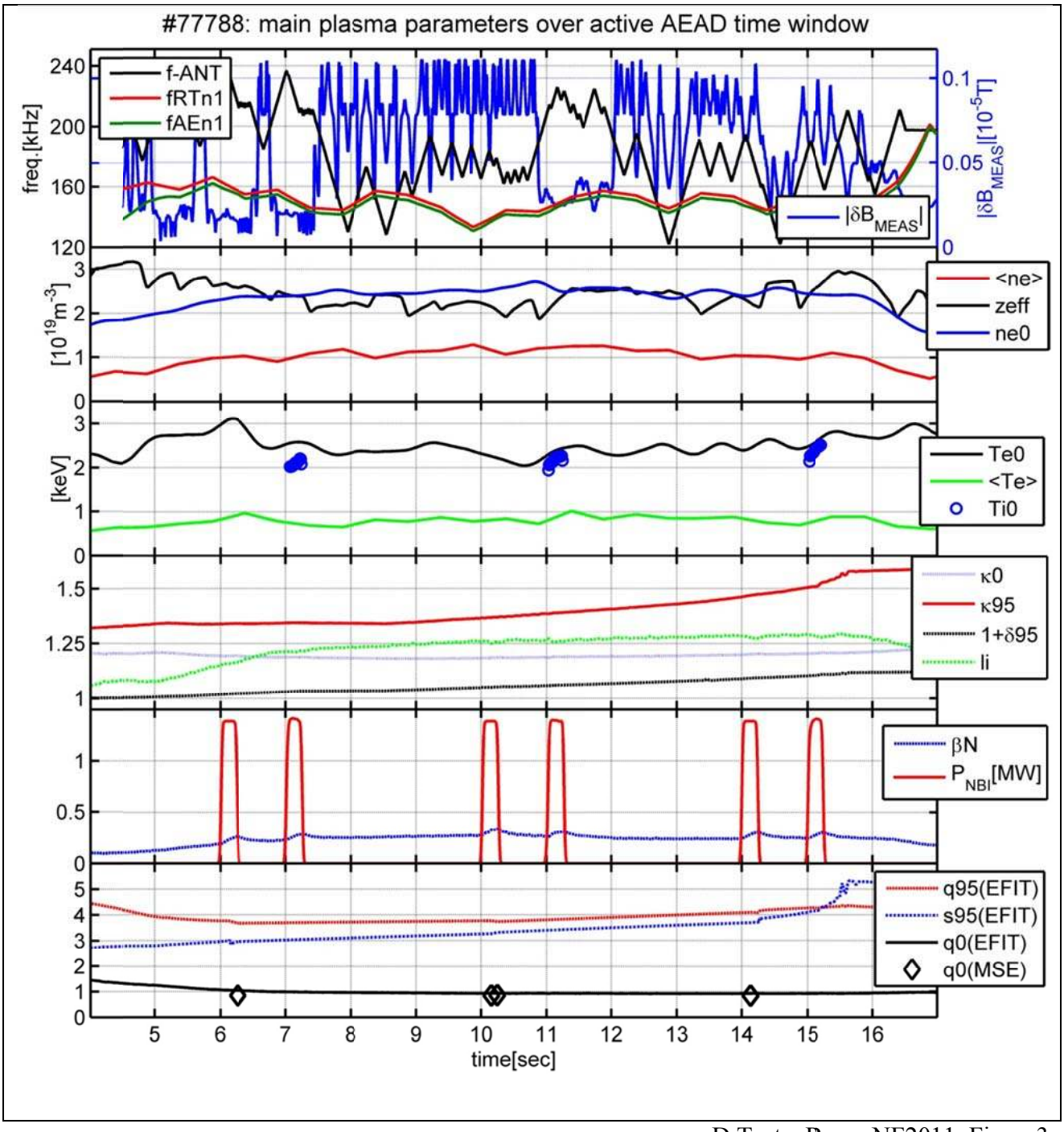

D.Testa, Paper NF2011, Figure3

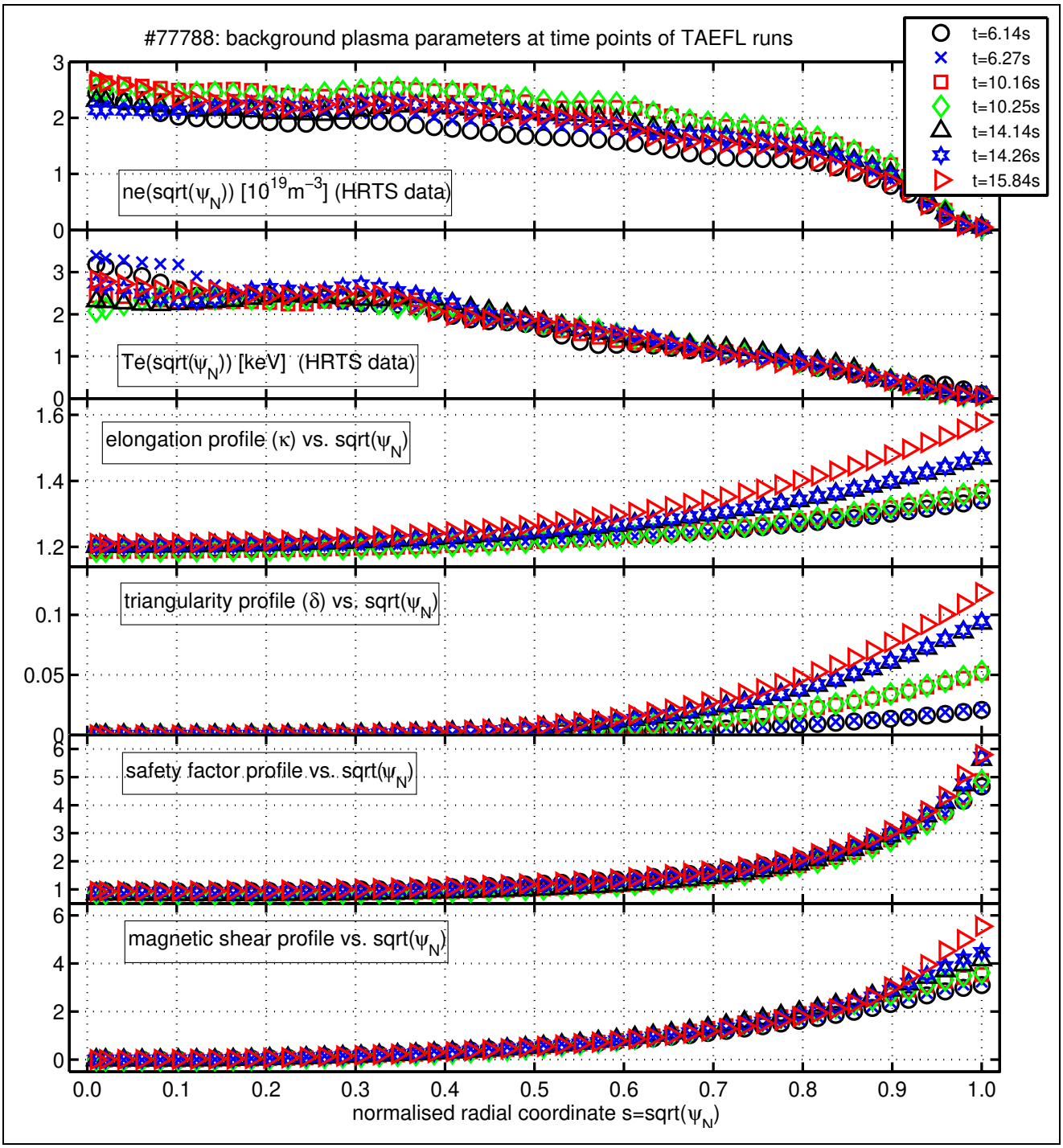

D.Testa, Paper NF2011, Figure4

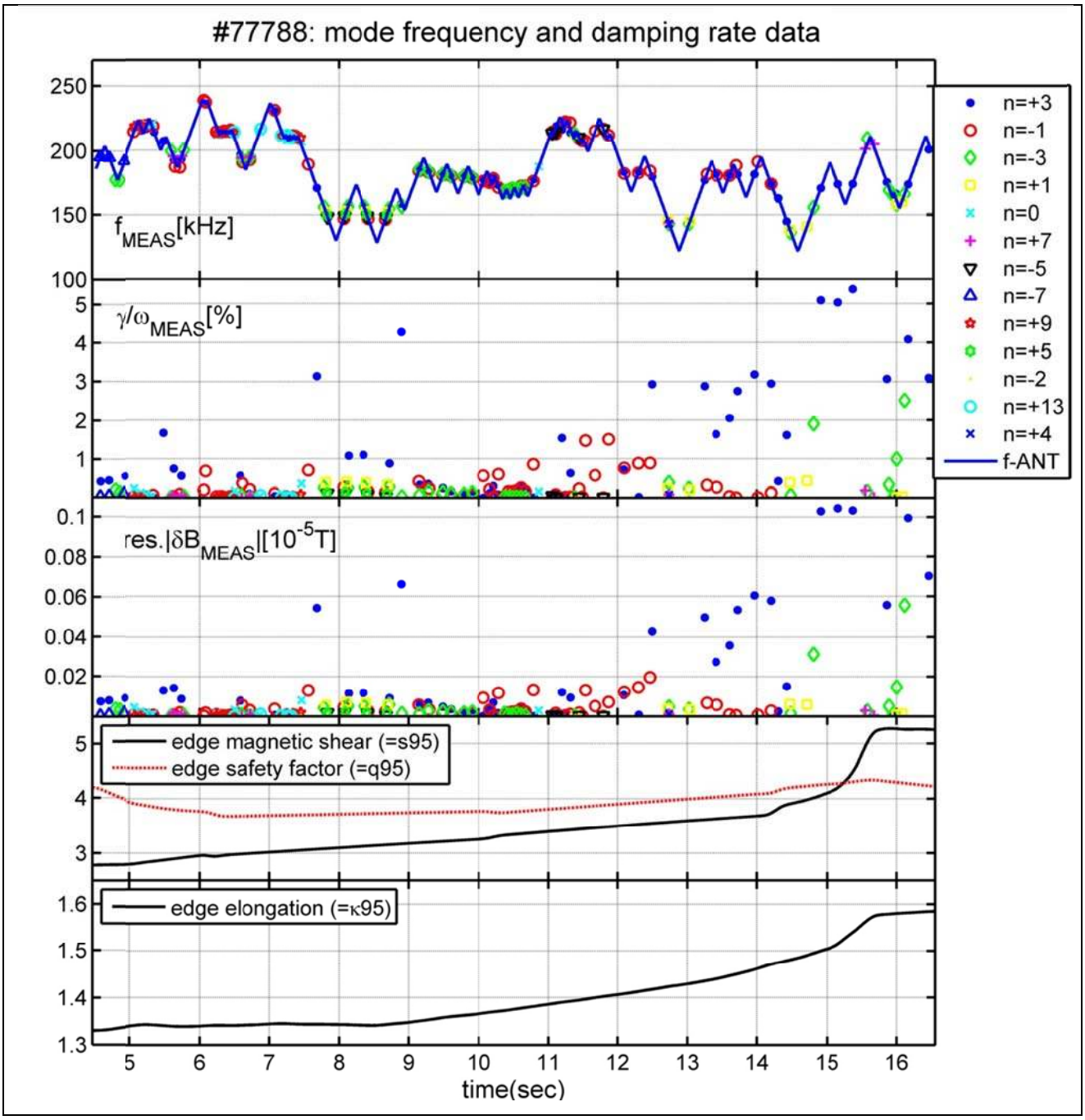

D.Testa, Paper NF2011, Figure5

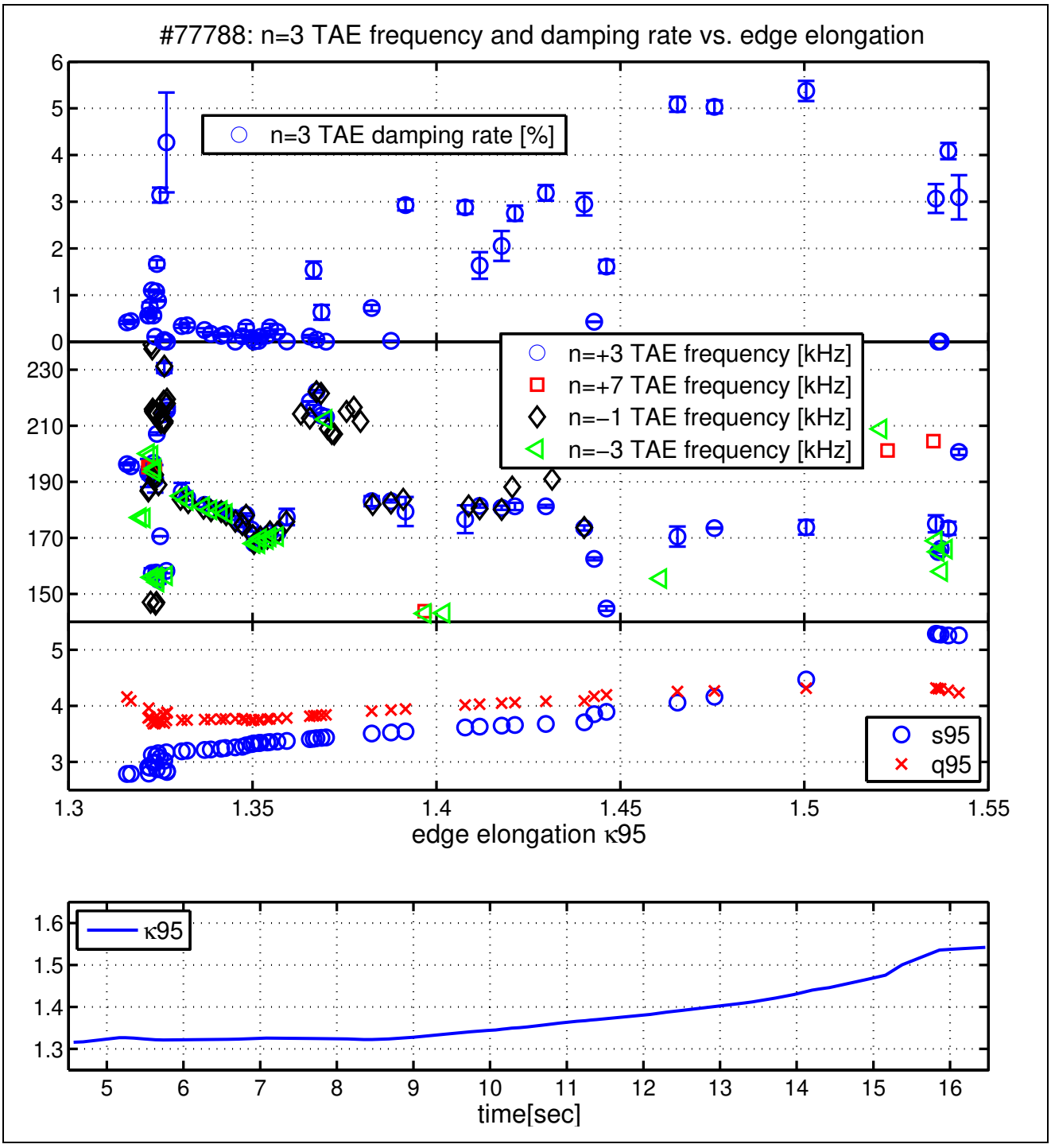

D.Testa, Paper NF2011, Figure6

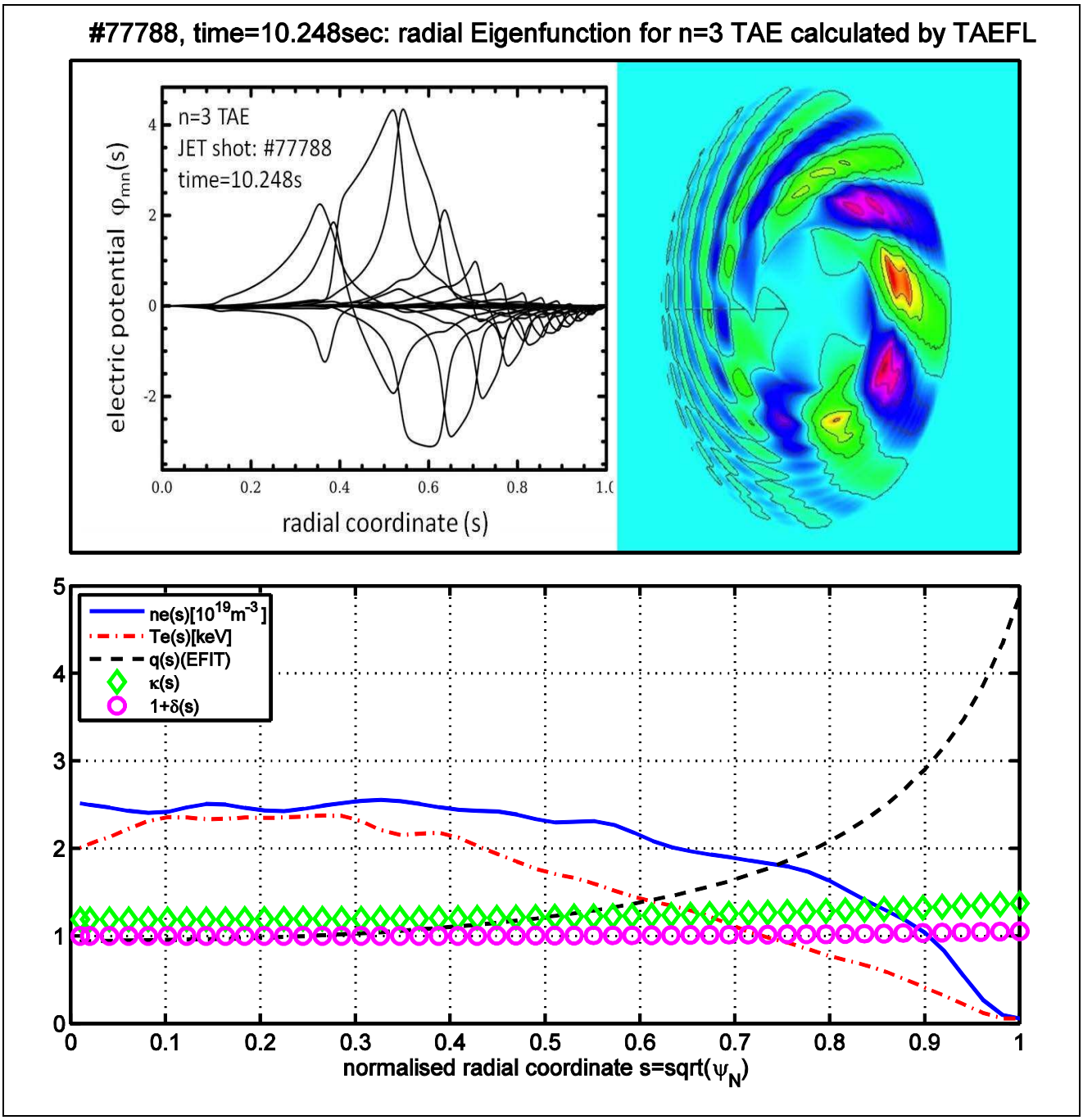

D.Testa, Paper NF2011, Figure7a

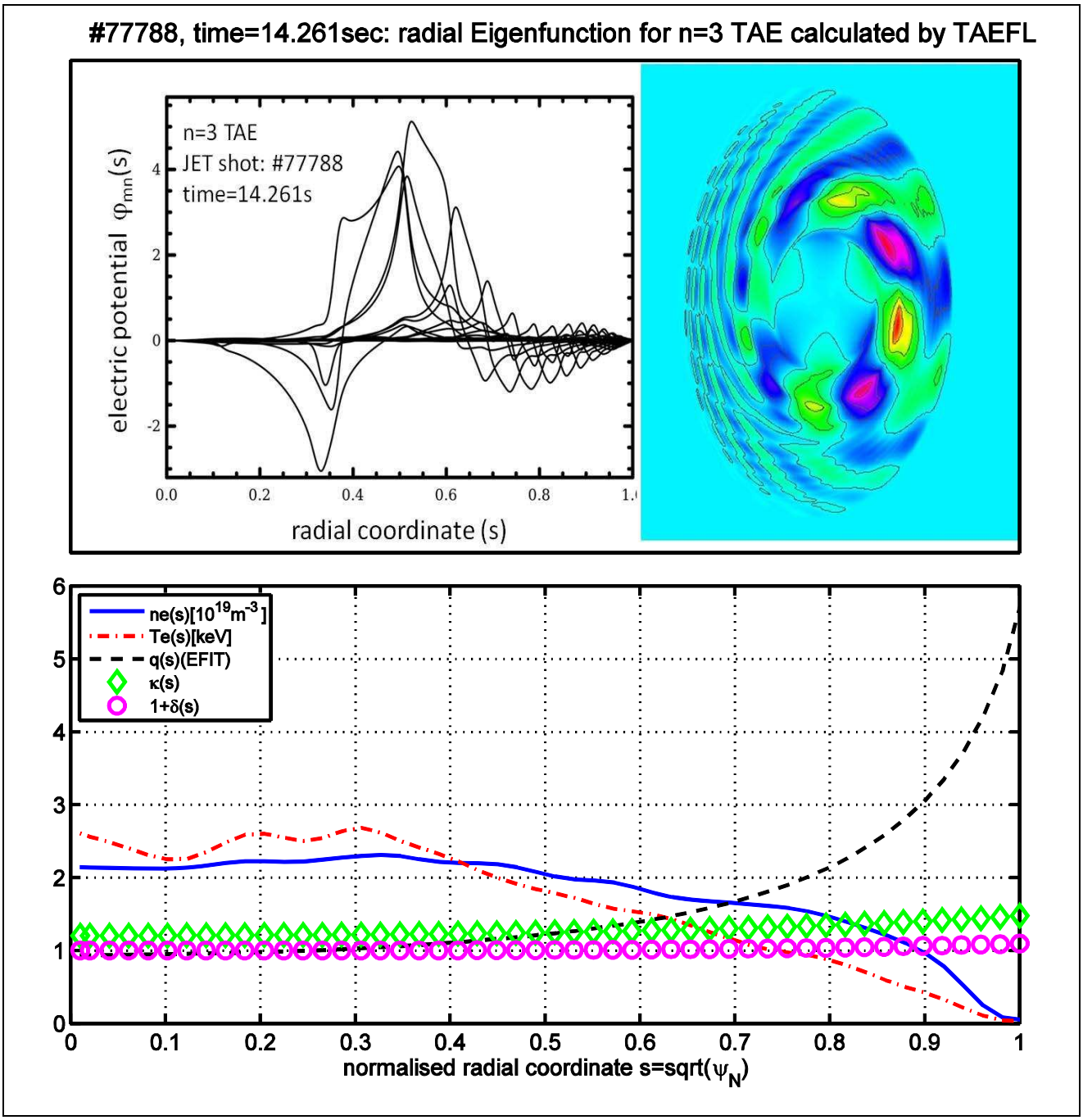

D.Testa, Paper NF2011, Figure7b

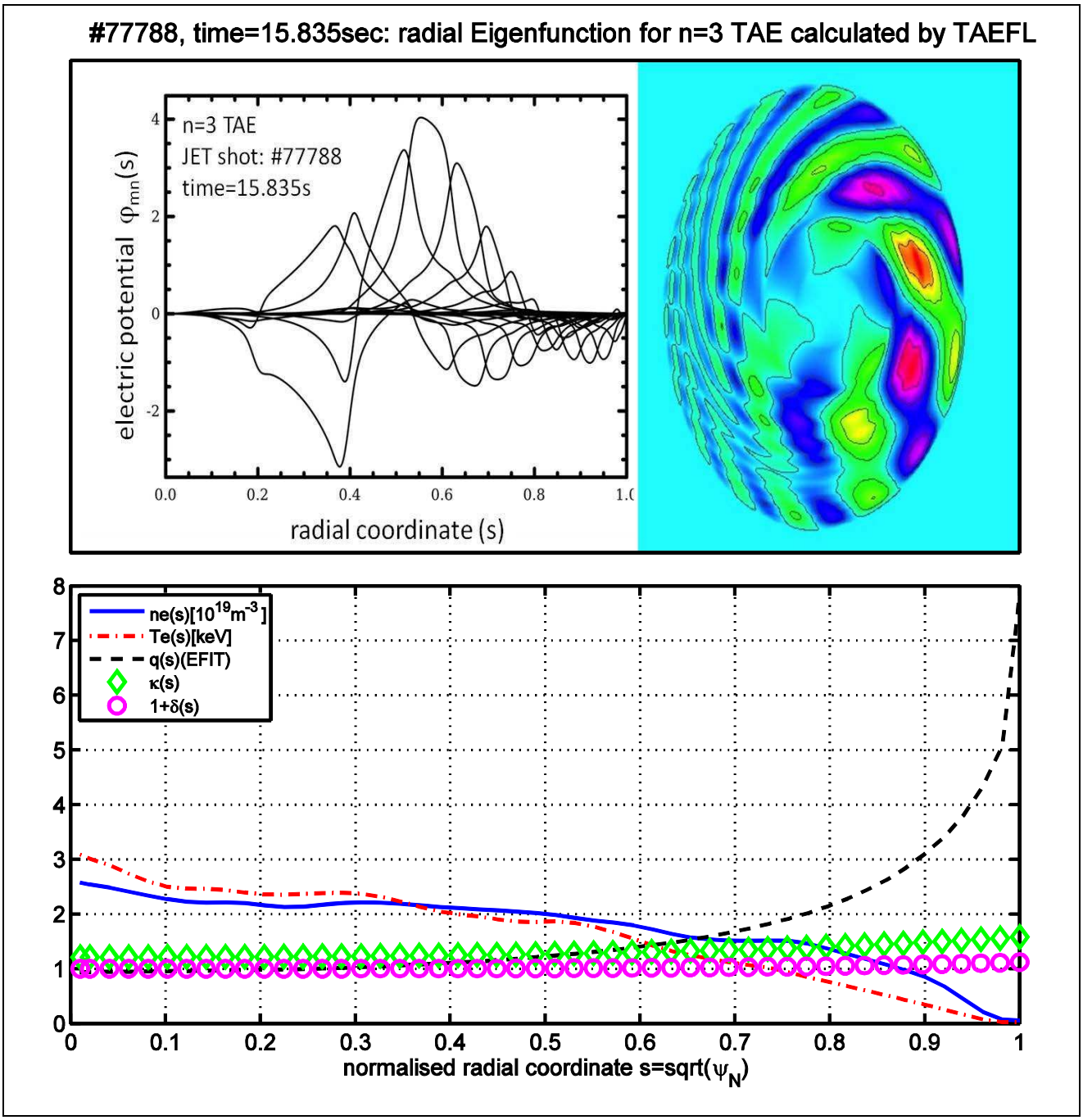

D.Testa, Paper NF2011, Figure7c

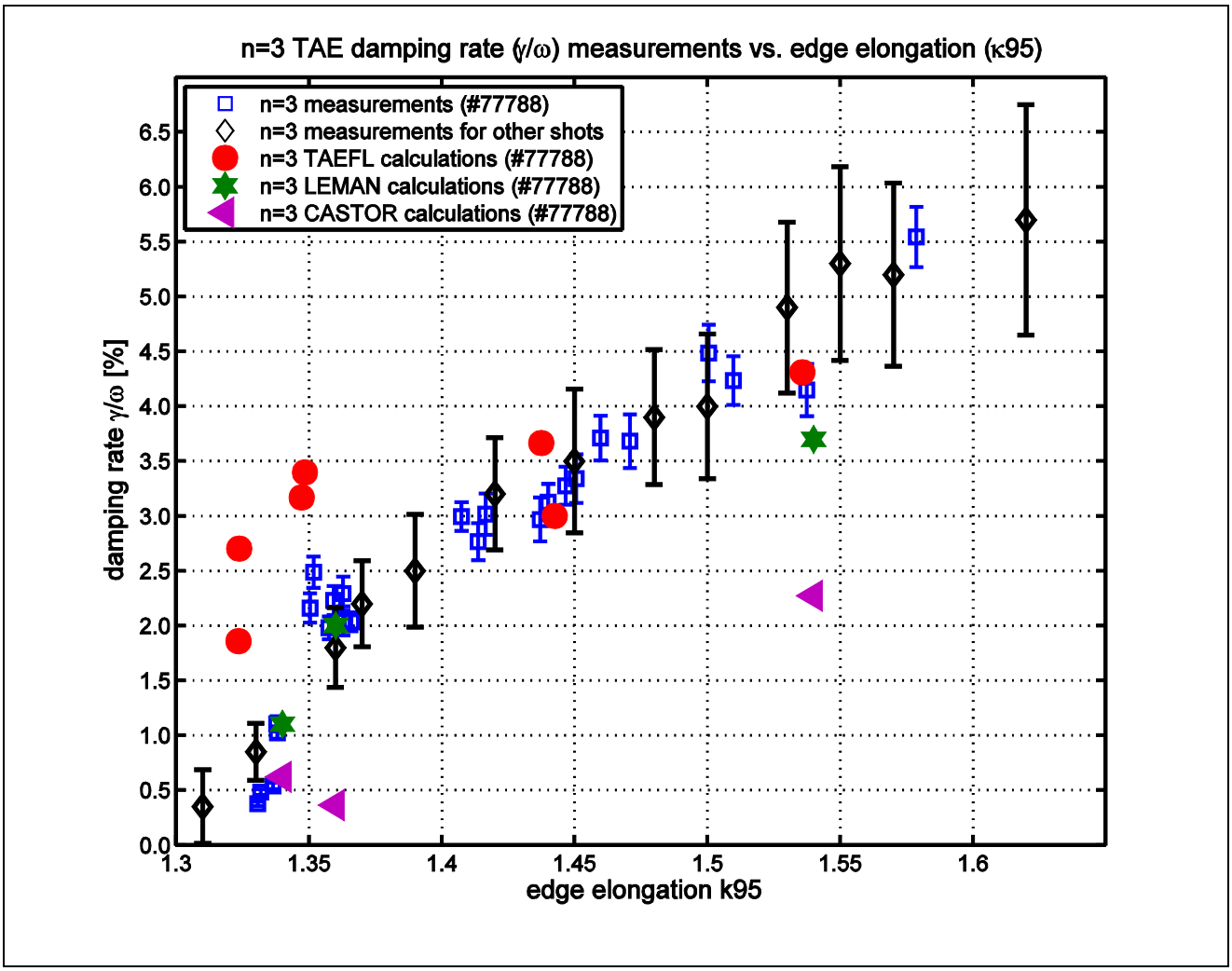

D.Testa, Paper NF2011, Figure8